Carbon 113 (2017) 340–345

Contents lists available at ScienceDirect

Carbon

journal homepage: www.elsevier.com/locate/carbon

Localized resistance measurements of wrinkled reduced graphene oxide using *in-situ* transmission electron microscopy

Hanna M. Nilsson [a, b], Ludvig de Knoop [a], John Cumings [b], Eva Olsson [a, *]

[a] Department of Physics, Chalmers University of Technology, 412 96, Gothenburg, Sweden
[b] Department of Material Science and Engineering, University of Maryland, College Park, 20742, MD, USA

ARTICLE INFO

Article history:
Received 25 July 2016
Received in revised form
25 October 2016
Accepted 26 October 2016
Available online 27 October 2016

ABSTRACT

The tunable electrical properties of reduced graphene oxide (rGO) make it an ideal candidate for many applications including energy storage. However, in order to utilize the material for applications it is essential to understand the behavior of the material on the nanoscale, especially how naturally occurring phenomena like wrinkling affect the electronic transport. Here, we use a transmission electron microscope (TEM) with electrical probe *in-situ* holder to perform localized electrical measurements on wrinkled, supported rGO flakes. The TEM allows for observation of the local wrinkled structure of the rGO and simultaneously an electrical probe is used to perform localized resistance measurements. For these measurements, there is no correlation between the electrode distance and the measured resistance indicating that contact resistance varies and dominates the measurements. There is, however, a correlation between increasing number of wrinkles underneath the probe and decreasing resistance, indicating that the wrinkles can provide surface area for contact with the probe and thus lower the resistance. The overall resistance is on the order of single kΩ, if the contact between the probe and the rGO is optimized. These measurements give evidence that rGO with wrinkling can compete as a leading type of graphene for certain applications.

1. Introduction

The reduction of graphene oxide (GO) has been suggested as a route towards both large-scale production of graphene [1] and as a way to tune the electronic properties of the material [2,3]. The most well-studied form of graphene may be chemical vapor deposition (CVD) grown graphene [4], however, despite many years of work, large scale production of graphene using this method does not yet seem economically viable for most applications, thus opening up an opportunity for reduced GO (rGO) to become the material of choice in future electronics and energy storage applications. While graphene is a zero bandgap semiconductor and GO is an insulator, the reduction of GO either by chemical or thermal means, allows for the creation of a material with tunable semimetal or semiconductor properties [5,6]. This makes rGO a promising candidate for applications such as supercapacitors, batteries, and solar cells [7,8]. While theoretical modeling of this material have come a long way in understanding the mechanism of the electron transport as a function of reduction [9,10], less work has been performed measuring the performance of this material in realistic device situations. Thus far there is consensus that the electron mobility of rGO is lower than pristine graphene due to a large amount of sp^3 carbon left from the reduction process [11,12], but some studies suggest that rGO is more robust against extrinsic influences, such as temperature and substrate material [13].

One issue that becomes important when incorporating the material into devices is the formation of wrinkles [14,15]. There have been both theoretical [16] and experimental studies on the effect of wrinkles on the electrical conduction of different types of graphene; GO [17], rGO [18], and pristine, with varied results [19]. Theoretical predictions suggest that wrinkles create additional scattering sites that reduce the electrical conductivity [20], which are confirmed by some localized scanning probe measurements [18,19,21]. However, other measurements of sheets containing wrinkles are inconclusive or point toward no negative influence from wrinkles [15,22,23]. Zhu et al., for example, find that there is anisotropy when looking at the resistance change caused by wrinkles in exfoliated graphene, with measurements along a fold showing lower resistance than control samples without wrinkles,

* Corresponding author.
E-mail address: eva.olsson@chalmers.se (E. Olsson).

http://dx.doi.org/10.1016/j.carbon.2016.10.086

and measurements across a fold showing the same resistance as control samples without wrinkles [22]. Deshpande et al. mapped the Dirac point in chemical vapor deposition (CVD) graphene using scanning tunneling microscopy (STM) and came to the conclusion that there is no correlation between topographical features such as ripples and the electronic structure [23]. A common denominator for many of these measurements is that they either test the entire structure without control of the local structure or they rely only on information obtained from a probe in contact with the graphene. Here, in order to improve the accuracy and control of measurements, we perform transmission electron microscopy (TEM) imaging while simultaneously performing electrical probing measurements. The literature contains limited amount of data for each type of graphene so comparisons must be made between the types rather than within a certain type. However, these comparisons between, for example CVD and rGO, are also valuable as graphitic materials move closer to application ready and choices must be made as to which material is best for each application. We argue that rGO is a better choice than CVD graphene for applications where wrinkles and large contact area ratios are beneficial, such as for catalysts and composite materials. In addition, rGO has more promise in large-scale cost-effective production compared to CVD graphene [8,24].

2. Experimental methods

2.1. Materials preparation

The rGO used in this study was purchased from Angstrom Materials. The product name is "Nano Graphene Platelets." They report ≥95.00 wt% carbon, ≤2.00 wt% hydrogen, ≤0.50 wt% nitrogen, ≤2.50 wt% oxygen, and ≤2.50 wt% ash. The graphene powder is suspended in 1 wt% ammonium laurate (AL) surfactant and is then probe sonicated for 10 min (1 s on/1 s off) at 100 W to disperse the material evenly in solution. This is followed by 15 min of centrifugation at 4000 rpm and decanting the top 50% in order to remove the heavier unwanted particles. The sample membranes used are 50 nm thick SiN TEM windows with 8 Au electrodes. The membranes are plasma cleaned and then left in the rGO solution over night. When they are taken out in the morning they are rinsed with DI water to remove any left over surfactant. The samples are then silver glued (CircuitWorks CW2400) to Au posts so that all of the electrodes can be connected to the bias on a Nanofactory Instruments *in-situ* TEM-STM holder. This glue has a reported resistance of <0.001 Ω-cm. We measure the resistance to be around 2 Ω from the Ag glue to the sample holder.

2.2. Experimental set-up

We employ simultaneous TEM imaging and probe manipulation for optimal control of the local structure during resistance measurements of rGO. The *in-situ* TEM probe holder not only allows us to perform electronic measurements, but it also allows for mechanical manipulation of the structure. Fig. 1 shows an optical microscope image and schematic of the experimental set-up. Silicon nitride membranes with lithographically patterned Au electrodes are used as substrates. rGO flakes are deposited onto the substrates via an ammonium laurate surfactant by leaving the samples in solution overnight [25]. This means that the rGO is simply resting on top of the electrode rather than top-deposited metal, as is common [26]. The sample and a Au tip are then mounted opposite each other in the *in-situ* TEM sample holder (Fig. 1a). The sample's electrode pads are connected to the holder bias using Ag glue and a grounded Au tip is used to probe the sample locally. The TEM that was used is an FEI Tecnai T20 operated at 200 kV with a LaB6 gun.

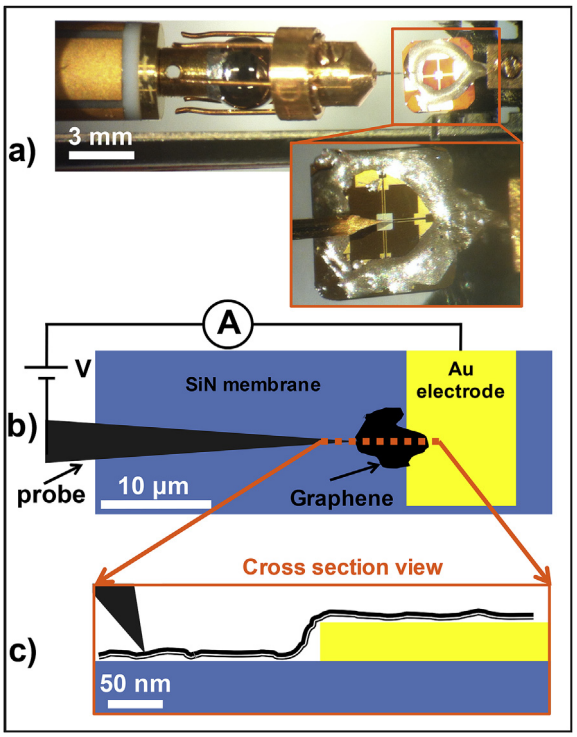

Fig. 1. Experimental set-up. a) Optical microscope image of Nanofactory *in-situ* TEM holder mounted with a patterned SiN membrane and a Au tip. The sample is connected to the holder bias via Ag glue and the Au tip is used to manipulate rGO on the SiN substrate and to perform local electric measurements. b) Top-view schematic of the circuit when the Au tip is used to bias rGO deposited onto Au electrodes. c) Side-view schematic of rGO resting on Au electrodes and SiN substrate while being contacted by a Au probe for electrical and mechanical manipulation.

3. Results and discussion

3.1. Resistance measurements

TEM imaging of these samples allows for locating rGO sheets in contact with Au electrodes and subsequently characterizing their structure. Fig. 2 show a typical TEM image of the rGO that was used in this study. These micron sized flakes were then contacted with the Au probe in multiple different areas for electrical biasing, typically from −1 V to +1 V and then back down to −1 V. Fig. 2 also highlights the method used to estimate the number of wrinkles under the probe at each measurement position. In addition, the distance between the probe and the electrode was recorded for each measurement. The measured total resistance values for this system varies greatly, most are in the 10s of kΩ, which is in accordance with previous literature values for rGO [2,3,27], but some as low as single kΩ and some as high as 100s of kΩs. It would be expected that there would be a correlation between the measured resistance and the distance between the probe and the electrode, but this is not the case here since the contact between the probe and the rGO varies for each measurement. A plot of the resistance as a function of the distance showing that there is no correlation between these two variables is provided in the Supplemental Material in Figs. S1 and S2. The variable that does show correlation to the measured resistance is the number of wrinkles counted under the probe during the measurement, as can be seen in Fig. 3c and will be discussed further below.